

Photoluminescence from mechanically milled Si and SiO₂ powders

T. D. Shen *

Department of Materials Science and Engineering, North Carolina State University, Raleigh, North Carolina 27695-7907

I. Shmagin

Department of Electrical and Computer Engineering, North Carolina State University, Raleigh, North Carolina 27695-7911

C. C. Koch

Department of Materials Science and Engineering, North Carolina State University, Raleigh, North Carolina 27695-7907

R. M. Kolbas

Department of Electrical and Computer Engineering, North Carolina State University, Raleigh, North Carolina 27695-7911

Y. Fahmy

Department of Materials Science and Engineering, North Carolina State University, Raleigh, North Carolina 27695-7907

L. Bergman and R. J. Nemanich

Department of Physics, North Carolina State University, Raleigh, North Carolina 27695-8202

M. T. McClure and Z. Sitar

Department of Materials Science and Engineering, North Carolina State University, Raleigh, North Carolina 27695-7907

M. X. Quan

State Key Lab of RSA, Institute of Metals Research, Academia Sinica, 72 Wenhua Road, Shenyang 110015, People's Republic of China

(Received 30 September 1996)

The photoluminescence (PL) in as-received and milled Si and SiO₂ powder is reported. The Si and SiO₂ powder is characterized by chemical analysis, Raman scattering, x-ray photoelectron spectra, infrared absorption, x-ray diffraction, and differential thermal analysis. The results indicate that the Si powder has amorphous Si oxide and suboxide surface layers. The milling of Si powder results in the formation of nanocrystalline/amorphous Si components. An amorphous SiO₂ component is formed by milling crystalline SiO₂. The PL spectra for as-received Si, milled Si, and SiO₂ powder exhibit similar peak shapes, peak maxima, and full width at half maximum values. For both the as-received and the milled Si powder, experimental results appear to exclude mechanisms for PL related to an amorphous Si component or Si-H or Si-OH bonds, or the quantum confinement effect. Similarly, for milled SiO₂ powder mechanisms for PL do not appear related to Si-H or Si-OH bonds. Instead the greatly increased intensity of PL for milled SiO₂ can be related to both the increased volume fraction of the amorphous SiO₂ component and the increased density of defects introduced in the amorphous SiO₂ upon milling. It is suggested that the PL for as-received Si, milling-induced nanocrystalline/amorphous Si, and milled SiO₂ results from defects, such as the nonbridging oxygen hole center, in the amorphous Si suboxide and/or SiO₂ components existing in these powder samples. The PL measurement for milled SiO₂ is dependent on air pressure whereas that for as-received SiO₂ is not, suggesting that new emitting centers are formed by milling. [S0163-1829(97)00311-1]

I. INTRODUCTION

Si and SiO₂ are the core materials of the semiconductor industry. Since Canham's report¹ in 1990, there has been a great interest in the light emission from porous silicon¹⁻⁹ because of possible applications for light-emitting devices. Visible photoluminescence (PL) has also been found in ultrafine Si particles^{10,11} and nanocrystalline Si films.¹²⁻¹⁴ Different mechanisms or models have been proposed for the visible PL in porous Si, such as (1) a quantum size effect,^{1-4,14} (2) the presence of amorphous silicon,⁵ (3) emission from molecular species such as siloxene⁶ or polysilane,⁷ (4) the effect of silicon hydride,⁸ (5) the effect of the non-

bridging oxygen hole center (NBOHC),⁹ etc. It has also been indicated recently that the silicon oxides may play an important role in the PL of porous Si and nanocrystalline Si, e.g., the strongly oxidized porous Si and nanocrystalline Si samples show yellow/red and green/blue luminescence.¹⁵ It is believed that the green/blue luminescence may be associated with the adsorption of OH groups in the silica network,^{15,16} with the radiative recombination of excitons confined in the crystalline Si (*c*-Si) core in the crystallite,¹⁷ or with the siloxene and/or SiO₂ on porous Si surfaces.¹⁸ As for the yellow/red luminescence, it has been suggested that it may result from an O-terminated Si surface layer,¹⁷ from some light-emitting centers in the Si oxide films,¹⁹ from

Si-OH bonds,²⁰ or from quantum confinement effects of remnant Si walls of porous Si.¹⁸

As for the SiO₂, it is suggested that the SiO₂ itself cannot effectively emit light in the visible region due to its high band-gap energy (usually >8 eV). However, in the case of the existence of various forms of oxygen deficiency introduced either during preparation or by external irradiation,²¹ both crystalline and amorphous SiO₂ may have luminescence bands in the visible or UV region. The related PL bands have been reported at around 1.9, 2.2, 2.7, 3.1, and 4.3 eV.^{21–25} Many amorphous SiO₂ samples with different Cl and OH contents do not exhibit these PL bands before gamma irradiation.²¹

Recently, mechanical milling has been widely used to prepare nanocrystalline metallic materials.²⁶ It has also been found that mechanical milling may be used to obtain crystalline-to-amorphous and/or crystalline-to-nanocrystalline transformations for some semiconductor elements, e.g., Si (Refs. 27 and 28) and Ge.²⁹ The partial amorphization of SiO₂ induced by mechanical milling has been reported by Steinike *et al.*³⁰ Moreover, a recent report indicates that the Si-O-Si strained bond and paramagnetic defect centers may be induced in a vibrating ball mill or agate mortar and pestle.³¹

This paper presents a study of PL from milled Si and SiO₂ powders. We sought to investigate the PL of milled Si powder because (1) mechanical milling offers the possibility for production of large quantities of nanocrystalline materials for potential applications,²⁶ and (2) we wish to understand if the milling-induced nanocrystalline/amorphous structure of Si has an influence on the PL. We sought to study the PL of milled SiO₂ because the Si-O-Si strained bond and paramagnetic defect centers formed by mechanical milling of SiO₂ may play an important role in the PL of SiO₂.

II. EXPERIMENT

Commercial crystalline Si and SiO₂ powders purchased from CERAC Inc. of nominal purity of 99.9% and 99.5% and average particle size of 150 and 5 μm, respectively, were used as starting materials. In each milling experiment 2 g of powder were placed into a hardened tool-steel vial together with 20 g of 440C martensitic stainless-steel balls of diameter 6 and 8 mm. Mechanical milling was performed in a high-energy Spex-8000 shaker mill at ambient temperature. Si powder samples with different oxygen content ranging from 2.57 to 38.65 at. % were prepared by controlled milling time and atmosphere (argon or air). The SiO₂ powder was milled in an air atmosphere. The Si and SiO₂ powders were characterized by chemical analysis, x-ray diffraction (XRD), x-ray photoelectron spectroscopy (XPS), Raman scattering, infrared absorption, and differential thermal analysis (DTA) techniques in order to obtain information on chemical composition, phase, chemical bond, and strain of the powder samples. The measurements are also helpful for understanding the mechanism of PL for the Si and SiO₂ powder samples. The oxygen content of the Si powder was measured using a LECO TC-436 oxygen/nitrogen analyzer. The milling conditions and the oxygen content analysis for various Si samples are shown in Table I. X-ray diffraction was performed with a Rigaku Geigerflex diffractometer with Cu Kα

TABLE I. Sample, milling atmosphere, milling time, and oxygen content for Si powder. The open interval indicates the time interval at the end of which the milling vial was opened to air.

Sample	Milling atmosphere/open interval	Milling time (h)	Oxygen content (at. %)
Si-1-20h	air/1 h	20	38.65
Si-1-10h	air/1 h	10	22.66
Si-2-20h	air/2 h	20	28.79
Si-2-10h	air/2 h	10	14.93
Si-3-10h	air/3.3 h	10	10.36
Si-4-10h	argon/3.3 h ^a	10	5.50
Si-5-20h	argon ^b	20	4.12
Si-5-7.5h	argon ^b	7.5	2.83
Si-5-1.5h	argon ^b	1.5	2.57

^aThe milling vial was opened to air, then sealed in a glove box filled with argon gas before the subsequent milling.

^bThe milling vial was sealed in a glove box filled with argon gas and milled, without opening, for the time listed.

radiation ($\lambda=0.154$ nm) and a graphite monochromator. The XPS spectra were taken using the Mg anode ($h\nu=1256.6$ eV) and a CLAMII hemispherical energy analyzer from VG Microtech. The chamber pressure for all measurements was in the 10^{-9} -Torr range. In addition to the Si powders investigated, a Si(001) wafer that had been HF etched was added as a reference. The spectra were normalized identical peak intensities. Raman spectra were excited with 150 mW of the 514.5 nm line from an Ar ion laser, and the scattered light was dispersed with a U1000 ISA double spectrometer. Infrared absorption spectroscopic study was carried out in an IG-10 infrared spectroscope. About 0.5–1 mg of powder was used for each measurement. The DTA was performed on a Perkin-Elmer DTA instrument with flowing argon at a rate of 40 ml/min as purging gas. The heating rate was 40 K/min. The DTA was operated in differential scanning calorimeter mode in order to obtain the value of heat release. Powders (approximately 60 mg) were placed in an Al₂O₃ crucible for DTA scans.

Samples for the PL measurements were prepared by pressing the powders into indium on a copper heat sink. Photoexcitation measurements were performed using a continuous argon ion laser operating at a wavelength of 488 nm, and sample luminescence was measured using a 0.5-m spectrometer with a coupled S-1 photomultiplier. The PL measurements were performed under both a vacuum better than 0.1 Torr and air atmosphere (760 Torr).

III. RESULTS

A. Characterization of milled Si

The Raman spectra of various Si powder samples are shown in Fig. 1. The as-received Si [Fig. 1(a)] exhibits a relatively sharp peak with a maximum at 519 cm^{-1} and full width at half maximum (FWHM) of 7.3 cm^{-1} , associated with the well-known Raman-active mode of crystalline Si. The milled Si exhibits a shifted and broadened crystalline Raman peak with maximum and FWHM of 514 cm^{-1} and 15 cm^{-1} for Si-5-1.5h [Fig. 1(b)], and of $507\text{--}513\text{ cm}^{-1}$ and

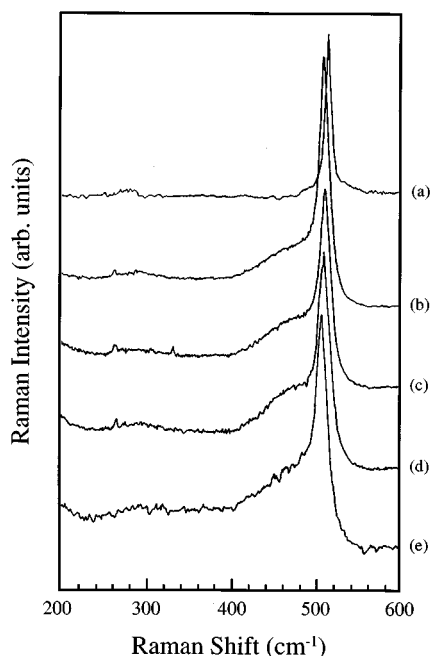


FIG. 1. Raman spectra of various Si powder samples. (a), as-received polycrystalline Si; (b), Si-5-1.5h; (c), Si-5-7.5h; (d), Si-5-20h; and (e), Si-2-10h.

$19\text{--}22\text{ cm}^{-1}$ for Si-5-7.5h [Fig. 1(c)], Si-5-20h [Fig. 1(d)], Si-2-10h [Fig. 1(e)], and all other samples listed in Table I. The shape for the spectra of various milled Si samples is similar. The milled Si also exhibits an additional broad lower-frequency peak with a maximum at around 480 cm^{-1} , which is attributed to an amorphous Si component.^{32,33} The coexistence of amorphous and nanocrystalline components in the milled Si powders has also been verified by other experimental techniques, such as high-resolution electron microscopy and differential scanning calorimetry, as reported previously.²⁸ The volume fraction of the amorphous Si component, as determined by the relation introduced by Nemanich *et al.*,³⁴ is 0%, 41%, and 50–57 % for as-received Si, Si-5-1.5h, and all other milled Si samples listed in Table I, respectively. The amorphous component estimated from the Raman spectra may include the disordered Si component located at the grain boundaries. Thus, the actual fraction of amorphous phase could be smaller than the value estimated from Raman spectra.²⁸ The domain size, i.e., crystallite size, can be estimated by the Raman linewidth and/or frequency shift of the Raman peak related to large-grained crystalline Si.³⁵ The estimated crystallite size is 5 nm and 4–4.3 nm for Si-5-1.5h and all other milled Si listed in Table I, respectively. The high-resolution electron microscopy images, however, indicate that there exists a distribution (3–20 nm) for the crystallite size in milled Si powders. Thus, the crystallite size estimated from the Raman spectra is an average value.

Displayed in Figs. 2(a) and 2(b) are the XPS spectra for as-received and milled Si powders. As shown in Fig. 2(a), curve (a), the as-received Si exhibits two peaks with maxima at around 99.2 and 103.3 eV. The XPS spectra for milled Si [Fig. 2(a), curves (b), (c), and (d)] and other Si samples listed in Table I are very similar, i.e., all of the spectra exhibit a higher-energy peak at around 103 eV and a lower-

energy peak at about 99.2 eV. The Si-1-20h sample only shows a peak with a maximum at around 103 eV. The XPS spectra with an energy range from 0 to 1200 eV (not shown) only indicate the existence of Si, oxygen, and carbon. No nitrogen peak is detectable. Comparing the present results with the XPS spectra for the Si-SiO₂ interface^{36–39} or Si oxide after ion implantation,⁴⁰ the lower-energy and higher-energy peaks shown in Fig. 2(a) can be well ascribed to Si⁰ and Si⁴⁺ states, i.e., elemental Si and SiO₂. The relative peak intensities between the Si 2*p* and the SiO₂ feature remained approximately the same for the as-received Si, Si-5-1.5h, and Si-3-10h samples. The amount of SiO₂ bonding increased for the Si-1-10h sample and all of the Si is incorporated into SiO₂, to the probing depth of XPS (~5 nm), for the Si-1-20h sample. It has also been indicated^{36–40} that the Si suboxide states, Si⁺, Si²⁺, and Si³⁺ characterized by bonding to one, two, or three oxygen atoms, can exist in the Si-SiO₂ interface^{36–39} or Si oxide after ion implantation. The difference between the binding energy for Si⁺, Si²⁺, and Si³⁺ states and that for the Si⁰ state (elemental Si) has been reported to be 0.6–1.86, 1.5–2.93, and 2.6–3.63 eV, respectively.^{36–40} The XPS peaks for these Si suboxide states exist in the spectral region between the Si and SiO₂ peaks. For the Si-1-10h sample, the broad width of the peaks suggest that additional, smaller peaks are present. The peaks present between the SiO₂ energy (103 eV) and the Si 2*p* energy (99.2 eV) would indicate that silicon suboxides are present. In fact, the spectra shown in Fig. 2(a), curves (b), (c), and (d) cannot be fitted by only the Si and SiO₂ peaks, regardless of whether the peak shape is Gaussian type or Lorentzian type as analyzed by a Micro Origin 4.0 peak-fitting procedure. This indicates that the spectra consist of a signal component related to Si suboxide spectra contributions between the Si and SiO₂ peaks.

The O 1s spectra, as shown in Fig. 2(b), reveal similar information. Some physisorbed oxygen and oxygen bonded to silicon are present for all of the silicon powder samples. Samples Si-5-1.5h, Si-3-10h, and Si-1-10h display a small peak around 529.5 eV corresponding to carbon-oxygen bonding, probably from atmospheric contamination. The high-peak intensity at 531 eV for sample Si-1-20h suggests that the majority of the oxygen present is integrated into SiO₂.

The as-received polycrystalline Si powder is composed of Si and a small amount of SiO₂. The SiO₂ component apparently exists near the surface region of the powder particles due to their exposure to air. The Si suboxide component may exist near the region of the Si/SiO₂ interface.^{36–39} However, the Si suboxide peak is not detectable in the XPS spectra of the as-received Si powder, indicating that the amount of Si/SiO₂ interface and the related Si suboxide component is very small. When the Si powder is milled, more SiO₂ and Si suboxide phases are formed. The increased amount of SiO₂ phases may be attributed to the fact that the milled Si has a much smaller particle size, about 0.5 μm as evidenced by the scanning electron microscopy observation,²⁸ when compared with the particle size, about 150 μm , of the as-received Si. Thus the amount of surface area and the related SiO₂ component increases. The increased amount of Si suboxide component may be related to the many Si/SiO₂ interfaces that are formed from the repeated cold welding and fracture occur-

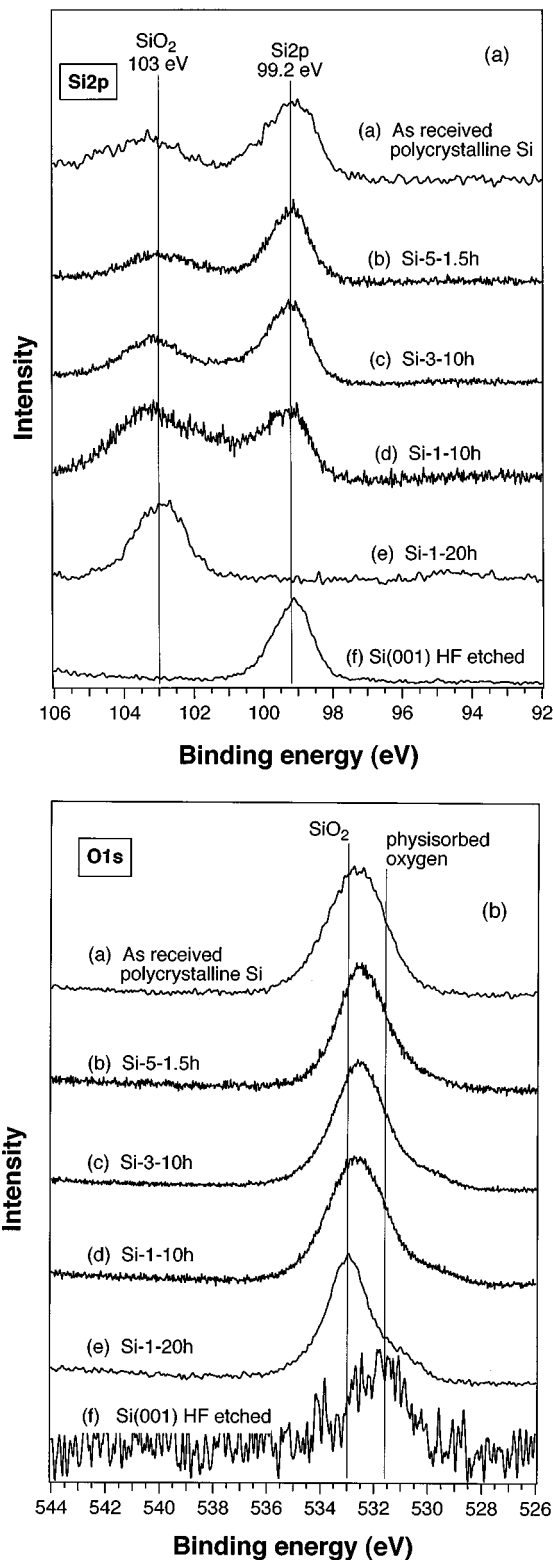


FIG. 2. (a) XPS spectra of the silicon $2p$ photoelectron energy region of (a), as-received polycrystalline silicon; (b), sample Si-5-1.5h; (c), Si-3-10h; (d), Si-1-10h; (e), Si-1-20 h; and (f), Si(001) after HF etching provided as a standard. The energies of interest are 99.2 eV for the Si $2p$ bonding and 103.0 eV for SiO₂. (b) XPS spectra of the oxygen $1s$ photoelectron energy region of (a), as-received polycrystalline silicon; (b), sample Si-5-1.5h; (c), Si-3-10 h; (d), Si-1-10h; (e), Si-1-20h; and (f), Si(001) after HF etching provided as a standard. The energies of interest are 531.5 eV for physisorbed oxygen and 531.0 eV for SiO₂.

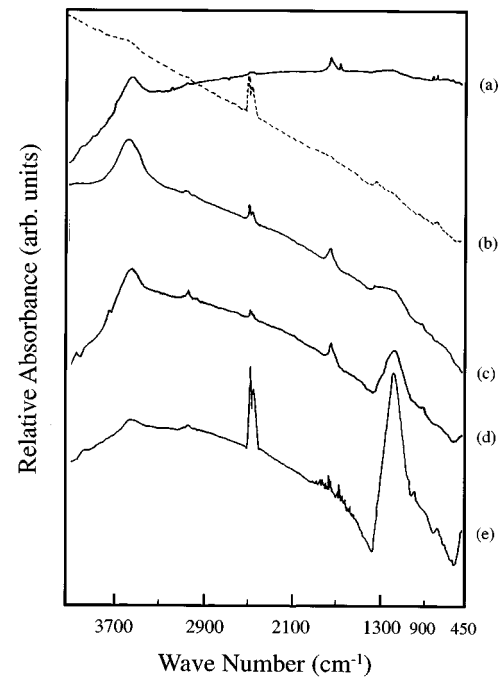


FIG. 3. Infrared absorption spectra for various Si powder samples. (a), as-received polycrystalline Si; (b), Si-5-1.5 h; (c), Si-3-10h; (d), Si-1-10h; and (e), Si-1-20h.

ring during the milling. Furthermore, more frequent exposure of Si to air during milling will result in a larger amount of Si suboxide component. This may be related to the fact that more SiO₂ and thus more Si/SiO₂ interfacial area will be formed.

Infrared spectra for various Si samples are shown in Fig. 3. It has been shown⁴¹ that the Si-O band exhibits a peak ranging from 980 to 1080 cm⁻¹ depending on the x value in SiO _{x} . It can be seen from Fig. 3 that a peak related to the Si-O band located near 1060–1070 cm⁻¹ (corresponding to SiO _{x} with a composition x of 1.71 and 1.84, respectively⁴¹) exists in the spectra for Si-3-10h, Si-1-10h, and Si-1-20h samples. Although the XPS spectra shown in Fig. 2 indicate that the Si-O band also exists in as-received Si and Si-5-1.5h powder samples, the Si-O mode peak does not appear in the IR spectra for these two samples. This suggests that the fraction of SiO₂ and SiO _{x} components in these two samples is too small to be detected in the IR spectra. The peaks at ~2335–2361 and ~1631–1636 cm⁻¹ could be related to CO₂ (Ref. 42) and C₃O₂ (Ref. 43) components, respectively. In fact, the XPS spectra (not shown) with a binding energy ranging from 0 to 1200 eV indicate that there is Si, O, and C elements in the as-received and milled Si powders. Additionally, the IR spectra for all of the samples investigated exhibit a peak at ~3400 cm⁻¹ that may be related to physically absorbed water.⁴⁴ There is no peak with frequency ranging from 3500 to 3746 cm⁻¹ for any of our samples, suggesting that there is no Si-OH bond.⁴⁴ Moreover, no peak with its position in the range from 2000 to 2190 cm⁻¹ was observed for any of the samples, indicating that the samples do not contain a Si-H _{n} ($n=1,2,3,\dots$) mode.⁴⁵

B. Characterization of milled SiO₂

Shown in Fig. 4 is the XRD patterns for mechanically milled SiO₂ powders. The as-received powders can be well

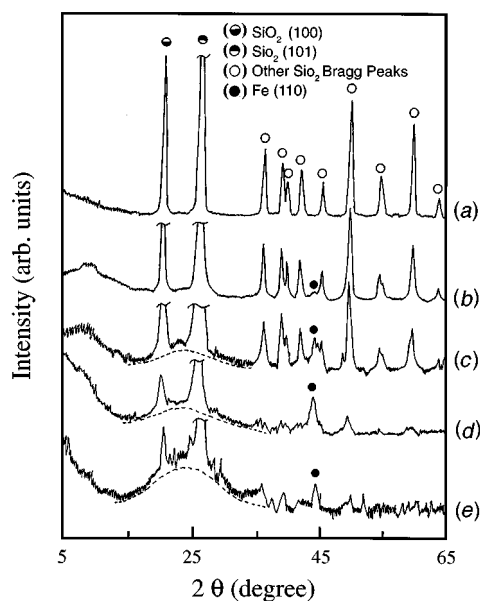


FIG. 4. XRD patterns for SiO₂ powder after (a), 0 h; (b), 20 min; (c), 50 min; (d), 3 h; and (e) 10 h of milling.

ascribed to hexagonal-structure crystalline quartz. Broadening of Bragg diffraction peaks with increased milling time is observed. The grain size, as calculated from the (101) Bragg reflection linewidth using the Scherrer formula⁴⁶ is approximately 14 and 13 nm for SiO₂ after 3 and 10 h of milling, respectively. A considerable amount of amorphous SiO₂ phase, with a broad diffuse peak between (100) and (101) reflections, appears for SiO₂ milled for 50 min, 3 h, and 10 h, as schematically indicated by the dashed lines shown in Fig. 4. We do not observe an amorphous peak in the SiO₂ milled for 20 min. This is because the XRD technique typically cannot detect an amorphous phase with volume fraction of less than approximately 5%. Additionally, Fig. 4 shows that the ball-milled SiO₂ powders contain a small amount of Fe due to Fe debris formed during milling.

The Raman spectra shown in Fig. 5 indicate that the as-received SiO₂ powders exhibit three peaks at around 200, 355, and 465 cm⁻¹, respectively, which can be attributed to the Si-O modes in crystalline SiO₂.⁴⁷ Upon milling for 20 min, only a weak peak at around 465 cm⁻¹ can be seen in the Raman spectra. The Raman spectra for SiO₂ after 50 min, 3 h, and 10 h do not reveal any peaks related to the crystalline SiO₂ structure over the frequency range from 100 to 600 cm⁻¹ but instead exhibit some weak signals that are not easily distinguishable from the background. It has been shown⁴⁷ that the Raman spectra of amorphous SiO₂ exhibit a very asymmetric and broad peak from about 150 to 580 cm⁻¹ with the peak maximum at about 430 cm⁻¹ while that of crystalline SiO₂ exhibits three relatively sharp peaks over the same frequency range. Moreover, the intensity of the peak maximum for amorphous silica is less than 10% of that for crystalline silica.⁴⁷ Furthermore, it has been indicated that the peak maximum at about 430 cm⁻¹ decreases with increasing stress.⁴⁸ Thus, the Raman spectrum for the SiO₂ powders after 50 min, 3 h, and 10 h of milling suggests that the milled SiO₂ powder consists of a relatively large amount

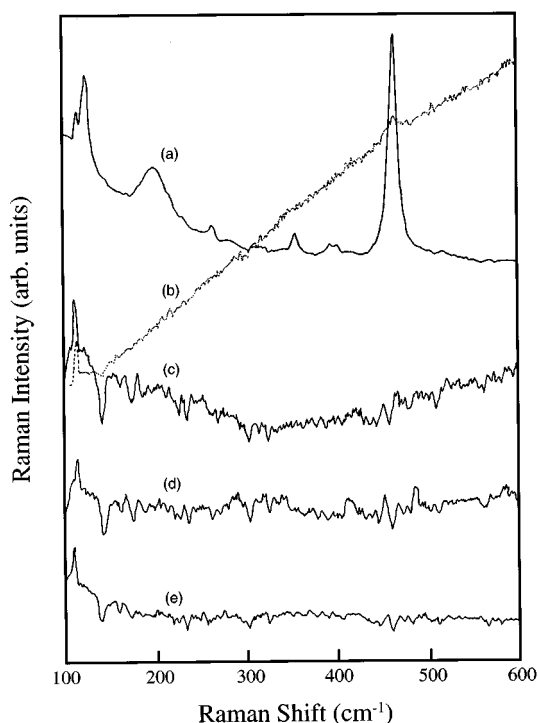


FIG. 5. Raman spectra for SiO₂ powder after (a), 0 h; (b), 20 min; (c), 50 min; (d), 3 h; and (e), 10 h of milling.

of amorphous structure that has been repeatedly subjected to high stresses induced by ball-powder-ball and ball-powder-wall collisions.

Shown in Fig. 6 is the infrared spectra for the as-received and milled SiO₂ powder. Three peaks at around 470, 776, and 1070 cm⁻¹ relate to the well-known rocking, bending, and stretching Si-O modes,⁴⁹ and one peak near 3400 cm⁻¹ related to physically absorbed water,⁴⁴ were observed. No spectral peaks were observed in the range of 2000–2190

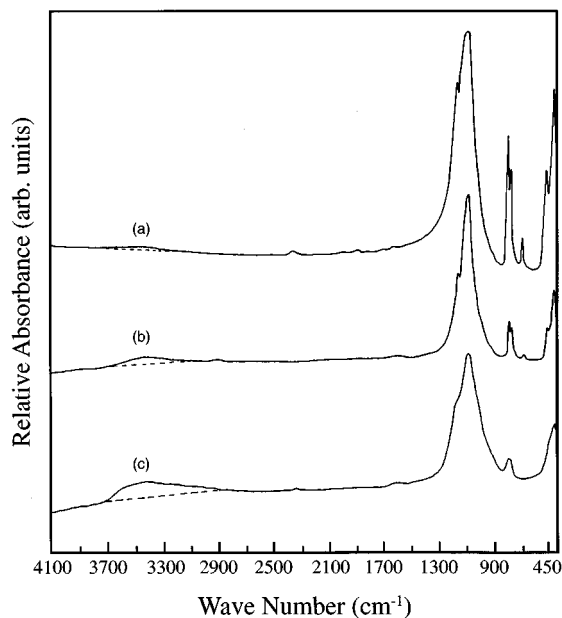


FIG. 6. Infrared spectra for SiO₂ powder after (a), 0 h; (b), 50 min; and (c), 10 h of milling.

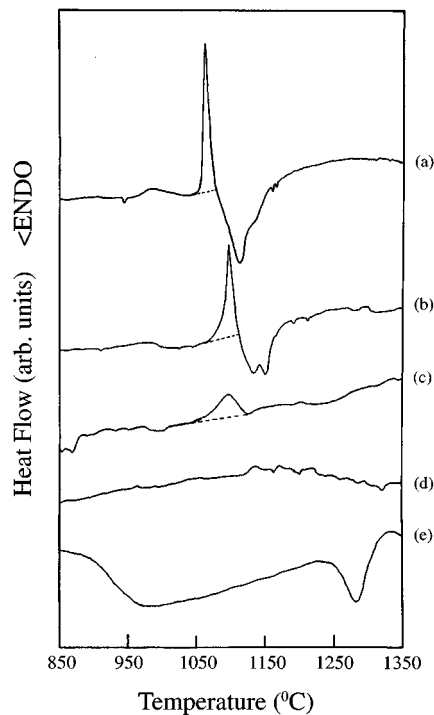


FIG. 7. DTA scans for SiO_2 powder after (a), 0 h; (b), 20 min; (c), 50 min; (d), 3 h; and (e), 10 h of milling.

cm^{-1} , indicating that the powders do not contain the Si-H_n ($n=1,2,3, \dots$) mode.⁴⁵ Also, no peaks were observed in the frequency range of $3520\text{--}3746\text{ cm}^{-1}$, suggesting that there is no Si-OH bonding.⁴⁴ Thus, the mechanism for PL related to Si-H or Si-OH bonds should not be applicable in the present case.

The DTA scans of SiO_2 samples are shown in Fig. 7. The as-received SiO_2 and SiO_2 milled for 20 min do not exhibit detectable exothermic peaks. The SiO_2 powder milled for 50 min, 3 h, and 10 h show an exothermic peak with a maximum at about 1108, 1113, and 1078 °C, respectively. The exothermic peak can be attributed to the crystallization of the amorphous SiO_2 component into crystalline SiO_2 . It has been reported^{50–52} that for amorphous SiO_2 crystallization begins at around 1000 °C. The direct evidence for the crystallization has been verified as follows. The XRD patterns for the SiO_2 powders milled for 10 h and heated to 1038 °C [below the exothermic peak shown in Fig. 7, curve (e)] in the DTA consist of a broad amorphous peak similar to that shown in Fig. 4. Once the SiO_2 powders milled for 10 h were heated to 1100 °C [above the exothermic peak shown in Fig. 7, curve (e)], the related XRD patterns show no broad peak related to an amorphous component but only peaks for the crystalline SiO_2 phases. Additionally, the relative amorphous volume fraction of the milled SiO_2 powders can be estimated from the heat release related to the crystallization peak. The heat release related to the crystallization peak shown in Fig. 7, curves (c), (d), and (e) was determined to be 7.0, 15.33, and 28.15 J/g, respectively. The volume fraction of amorphous SiO_2 component in the milled SiO_2 powders is proportional to the ratio of the heat of crystallization of milled SiO_2 powders to that of completely amorphous SiO_2 phases. Thus, the relative ratio of volume fraction of amorphous SiO_2 component for SiO_2 after 50 min, 3 h, and 10 h of milling is cal-

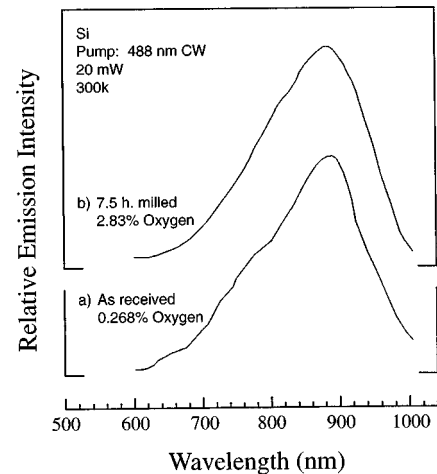


FIG. 8. PL spectra of Si powder measured in vacuum. (a), as-received polycrystalline Si (unmilled, 99.5% purity, 0.268 at. % oxygen content); (b), milled powder (7.5 h milling time, 2.83 at. % oxygen content).

culated to be 0.25:0.54:1. The absolute value of volume fraction of amorphous SiO_2 after milling cannot be estimated because the crystallization enthalpy of completely amorphous SiO_2 is not available in the literature.

C. PL from as-received and milled Si and SiO_2 powders

The photoluminescence spectra for (a) as-received polycrystalline Si (unmilled, 99.5% purity, 0.268% oxygen content) and (b) milled powder (7.5 h milling time, 2.83% oxygen content) are shown in Fig. 8. No light emission was detected from a bulk crystalline Si sample for the same intensity scale over the measured range from 660 to 1020 nm. All Si powders studied exhibited very similar photoluminescence spectra with peak positions at 890–900 nm (1.38–1.39 eV) and FWHM of 180 nm (0.31 eV).

The photoluminescence spectra for (a) as-received SiO_2 powder (unmilled); (b) 20 min; (c) 50 min; (d) 3 h; (e) 10 h milling times are shown in Fig. 9. The emission spectrum for as-received polycrystalline SiO_2 powder consists of two

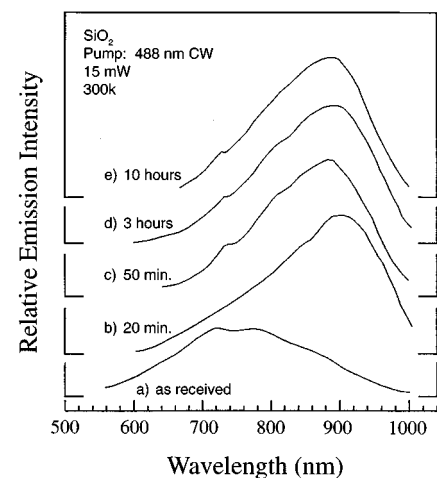


FIG. 9. PL spectra for (a), as-received SiO_2 powder (unmilled); (b), 20 min; (c), 50 min; (d), 3 h; (e), 10 h milling times.

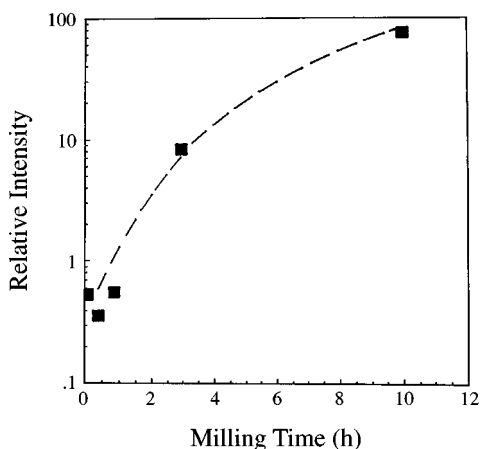


FIG. 10. Relative PL integrated intensity vs milling time for SiO_2 .

competing peaks at 730 (1.7 eV) and 780 nm (1.3 eV) with a combined FWHM of 230 nm (0.50 eV). The photoluminescence peaks shift to approximately 890 nm (1.39 eV) for the milled samples, and the FWHM changes to 180 nm (0.31 eV). A high-energy feature corresponding to 730 nm (1.7 eV) remains for all milled samples regardless of milling time and excitation energies. The overall integrated photoluminescence intensity increases by two orders of magnitude as the milling time is increased from 0 to 10 h as shown in Fig. 10.

All of the above-mentioned PL spectra were measured under a vacuum of 0.1 Torr. It was found that under excitation the PL from the as-received SiO_2 was stable both in air and vacuum and the luminescence appeared orange in color to the naked eye. The milled SiO_2 , however, exhibited no PL in air. The PL, appearing red in color, measured under vacuum for milled SiO_2 , was much less stable when compared with the PL measured under vacuum for as-received SiO_2 . The visible and IR photoluminescence would disappear and reappear when the milled SiO_2 powders were cycled between air atmosphere and vacuum.

IV. DISCUSSION

Raman spectra and the other experimental techniques reported previously²⁸ indicate that polycrystalline Si transforms into nanocrystalline/amorphous Si after mechanical milling. The shape, FWHM, and peak maximum of the PL spectra for as-received polycrystalline Si and milling-induced nanocrystalline/amorphous Si are very similar. There is no amorphous component in the as-received Si. Thus, PL from amorphous Si can be excluded as the source of the observed PL. The fact that the peak maxima for as-received polycrystalline Si and milled nanocrystalline/amorphous Si are similar indicates that the quantum confinement effect that might occur in nanocrystalline Si particles and porous Si could not be applicable to the PL of the milled Si powders. Otherwise, there should exist an obvious difference in the PL peak maximum for as-received polycrystalline Si and milled nanocrystalline/amorphous Si. For example, according to the relationship between PL peak energy and crystallite size suggested by Takagahara and Tokeda⁵³ the difference in PL peak maximum can be at least 190 nm for the as-received polycrystalline Si and milled Si with a

crystallite size of 5 nm as measured by the Raman linewidth, whereas the difference can be at least 385 nm for the as-received polycrystalline Si and the milled Si with a crystallite size of 4 nm as measured by the Raman linewidth. This large difference in peak position, however, has not been observed in the PL spectra for as-received and milled Si. Additionally, infrared spectra indicate that there are no Si-H or Si-OH bonds existing in the as-received and milled Si. Therefore, PL resulting from Si-H or Si-OH bonds in our samples can also be excluded.

Chemical analysis indicates that both the as-received Si powder and milled Si powder contain some amount of oxygen. The SiO_2 and Si suboxide phases existing in the various Si samples have been verified by XPS and infrared spectra. XPS is typically a surface analysis technique and the chemical information obtained is for the near-surface region with a probing depth of about 5 nm. The XPS spectra indicate that there exists a large amount of Si oxide and suboxide phases near the surface region of the powder particles even for the Si powder with an oxygen content of only 2.57 at. % (sample Si-5-1.5h). Thus, it is very possible that the PL for as-received and milled Si results from a similar origin, i.e., from the Si oxide and suboxide phases near the surface region of the Si powder particles. The high-resolution electron microscopy images for the Si powder milled in argon show an amorphous surface region up to 10 nm thick.²⁸ Combining this observation with the present XPS spectra, one can reasonably deduce that the surface region of Si powder particles is mainly amorphous Si oxide and suboxides. The Si suboxide is possibly concentrated near the interface of the Si oxide and Si.³⁶⁻³⁹ The bulk Si sample does not show a detectable PL peak whereas the as-received Si powder does, indicating that the PL peak can be detectable only when there exists a considerable amount of Si oxide and suboxide phases. In fact, the oxygen content of the as-received Si powder is about ten times that of the bulk Si sample. Moreover, the PL spectra from amorphous SiO_2 phases resulting from milling (to be discussed below) exhibit very similar spectra shape, position, and FWHM to those of the as-received and milled Si powders. This suggests that the PL may result from a similar light emission center in the near-surface amorphous Si oxide and suboxide phases of as-received and milled Si powder particles, and in the amorphous SiO_2 component of milled SiO_2 .

The excitation energy employed for the PL spectra measurement is 2.54 eV (488 nm Ar^+ laser), which is much lower than the band gap of SiO_2 (≈ 9 eV). Thus, the PL must result from direct excitation at defects. It is known²¹ that several kinds of defects, such as E' center, nonbridging oxygen hole center (NBOHC), and peroxy radical (E' center, NBOHC, and peroxy radical can be denoted as $\equiv\text{Si}\uparrow$, $\equiv\text{Si}-\text{O}\uparrow$, and $\equiv\text{Si}-\text{O}-\text{O}\uparrow$, respectively, where \equiv stands for the bonding with three separate oxygen atoms and \uparrow means an unpaired spin) exist in high-purity glasses and synthetic crystal α -quartz. The lowest energy for the PL peak in silica glasses has been reported to be in the 1.8–1.9 eV range that is believed to result from the NBOHC.^{54,55} The NBOHC induced PL has been recently used to explain the PL peak in the 1.7–1.8 eV range of porous Si.^{9,56,57} The PL for the as-received Si, milled Si, and SiO_2 could also result from such NBOHC defects. The PL peak energy for as-milled SiO_2 is at

~ 1.4 eV. This energy is ~ 0.4 – 0.5 eV less than the reported energy for silica glasses^{54,55} and ~ 0.3 – 0.4 eV less than the reported energy for the peak of PL induced by NBOHC.^{9,56,57} In fact, although the red luminescence band for porous Si has been generally reported to be in the 1.7–1.8 eV range, several groups have reported the luminescence band for porous Si at 1.44,⁵⁸ 1.5,⁵⁶ or ranging from 0.8–2.5 eV (Ref. 59) depending on the preparation and the subsequent treatment conditions. Thus, the slight redshift of the PL peak energy may be due to the special local environment of defects existing in the presently investigated powder. For example, the redshift of emission bands due to the small displacement of the O ion from its lattice site and strong interaction with the surrounding ions⁶⁰ has been theoretically predicted. The possible contribution of defects, such as NBOHC, to the PL of milled SiO₂ phases can further be verified as follows.

The illumination intensity of the SiO₂ sample milled for 10 h is about one order of magnitude higher than that for the sample milled for 3 h and two orders of magnitude higher than that of the sample milled for 50 min. However, the DTA analysis suggests that the volume fraction of the amorphous SiO₂ component in SiO₂ milled for 10 h is only two times that of the sample milled for 3 h and four times that of the sample milled for 50 min. This suggests that although the increasing volume fraction of the amorphous SiO₂ component on milling can enhance the illumination intensity for SiO₂, another factor may also make a considerable contribution to the greatly increased PL intensity of milled SiO₂. The enhancement in illumination intensity could be related to an increasing density of defects in the amorphous SiO₂ component induced by mechanical milling. The mechanical milling process results in repeated fracture and cold welding of the powder particles that induces plastic deformation in nominally brittle materials like SiO₂.²⁶ The amorphous SiO₂ component, once formed, will undergo such cyclic deformation upon further milling. The density of NBOHC defects was reported to exhibit an increase of about 10^{14} times for amorphous SiO₂ after 2 h of milling.⁶¹ Therefore, both the greatly increased density of NBOHC defects in amorphous SiO₂ regions formed upon milling and the growing volume fraction of the amorphous SiO₂ component could be responsible for the increasing intensity of PL for milled SiO₂ with milling time.

The atmosphere during measurement has an obvious influence on the PL behavior of milled SiO₂. The PL behavior for milled SiO₂ is similar to that for Si powder grown by plasma-enhanced chemical vapor deposition,⁶² i.e., the PL is only detectable under vacuum conditions of measurement and diminishes exponentially with the residual Ar or He gas pressure. It has been suggested⁶² that the existence of gas results in an interaction between the gas molecules and the emitting centers. Furthermore, the gas pressure exhibited an

obvious influence on the excited state lifetimes.⁶² Therefore, the completely different behaviors of atmospheric pressure dependence of PL for as-received and milled SiO₂ suggest that some new defects could be formed by milling SiO₂ powders. The new defects in SiO₂ induced by milling exhibit a strong interaction with gas whereas the defects in as-received SiO₂ do not. The fact that the PL peak energy and the related PL color are different for as-received and milled SiO₂ also suggests that new emitting centers are formed after milling. Further investigation is necessary to characterize the interaction between gas and emitting centers for SiO₂ powders.

V. SUMMARY

The structural characterization and PL of as-received and milled Si and SiO₂ powders have been studied. The as-received and milled Si powder have a surface region with an amorphous Si oxide and suboxide, the latter possibly existing in the Si/SiO₂ interface. The milling of crystalline Si results in the formation of nanocrystalline Si with a crystallite size of about 4–5 nm, and an amorphous component. The milling of crystalline SiO₂ results in the formation of partially amorphous SiO₂. The mechanisms for PL related to the quantum confinement effect, an amorphous Si component, Si-H, or Si-OH bond are excluded by the comparisons of the PL, Raman, and infrared spectra for as-received crystalline Si and those for milling-induced nanocrystalline/amorphous Si. The PL intensity of SiO₂ powder exhibits a shift in peak position and a large increase after milling. This may be related to both the formation of an amorphous SiO₂ component and the greatly increased density of defects in the amorphous SiO₂ component upon milling. The PL associated with Si-H or Si-OH bond for milled SiO₂ is excluded because of the infrared spectra results. In view of the fact that the PL spectra for as-received Si, milling-induced nanocrystalline/amorphous Si, and milled SiO₂ are similar, and that the common structural feature for all of these powder samples is the existence of amorphous Si suboxide and/or SiO₂ components, we suggest that defects, such as NBOHC, in amorphous Si suboxide and/or SiO₂ components could be responsible for the observed PL for as-received crystalline Si, milling-induced nanocrystalline/amorphous Si, and milled SiO₂ powder. The influence of atmospheric pressure on the PL for as-received and milled SiO₂ is completely different, suggesting that new defects acting as emitting centers may be formed during the milling.

ACKNOWLEDGMENTS

This work was supported by the U.S. National Science Foundation under Grant No. DMR-9203479 and by the National Natural Science Foundation of China.

*Present address: Center for Materials Science, MS K765, Los Alamos National Laboratory, Los Alamos, New Mexico 87545.

¹L. T. Canham, *Appl. Phys. Lett.* **57**, 1046 (1990).

²V. Lehmann and U. Gosele, *Appl. Phys. Lett.* **58**, 586 (1991).

³M. Yamamoto, R. Hayashi, K. Tsunetomo, Y. Osaka, and K. Kohno, *Jpn. J. Appl. Phys.* **30**, 136 (1991).

⁴B. Delley and E. F. Steigmeier, *Phys. Rev. B* **47**, 1397 (1993).

⁵R. P. Vasquez, R. W. Fathauer, T. George, A. Ksendzov, and T. L. Liu, *Appl. Phys. Lett.* **60**, 1004 (1992).

⁶M. S. Brandt, H. D. Fuchs, M. Stutzmann, J. Weber, and M. Cardona, *Solid State Commun.* **81**, 307 (1992).

⁷S. M. Prokes, O. J. Glembocki, V. M. Bermudez, R. Kaplan, L. E. Friedersdorf, and P. C. Searson, *Phys. Rev. B* **45**, 13 788 (1992).

⁸C. Tsai, K. H. Li, D. S. Kinosky, R. Z. Qian, T. C. Hsu, J. T. Irby,

- S. K. Banerjee, A. F. Tasch, J. C. Campbell, B. K. Hance, and J. M. White, *Appl. Phys. Lett.* **60**, 1700 (1992).
- ⁹S. M. Prokes, *Appl. Phys. Lett.* **62**, 3244 (1993).
- ¹⁰P. D. Milewski, D. J. Lichtenwalner, P. Mehta, A. I. Kingon, D. Zhang, and R. M. Kolbas, *J. Electron Mater.* **23**, 57 (1994).
- ¹¹H. M. Morisaki, F. W. Ping, H. Ono, and K. Yazawa, *J. Appl. Phys.* **70**, 1869 (1991).
- ¹²M. Rückschloss, B. Landkammer, and S. Veprek, *Appl. Phys. Lett.* **63**, 1474 (1993).
- ¹³M. Rückschloss, O. Ambacher, and S. Veprek, *J. Lumin.* **57**, 1 (1993).
- ¹⁴Xinwei Zhao, Olaf Schoenfeld, Junichi Kusano, Yoshinobu Aoyagi, and Takuo Sugano, *Jpn. J. Appl. Phys.* **33**, L649 (1994).
- ¹⁵Hideki Tamura, Markus Rückschloss, Thomas Wirschem, and Stan Veprek, *Appl. Phys. Lett.* **65**, 1537 (1994).
- ¹⁶M. Rückschloss, Th. Wirschem, H. Tamura, G. Ruhl, J. Oswald, and S. Veprek, *J. Lumin.* **63**, 279 (1995).
- ¹⁷Y. Kanemitsu, T. Futagi, T. Matsumoto, and H. Mimura, *Phys. Rev. B* **49**, 14 732 (1994).
- ¹⁸S. L. Zhang, F. M. Huang, K. S. Ho, L. Jia, C. L. Yang, J. J. Li, T. Zhu, Y. Chen, S. M. Cai, A. Fujishima, and Z. F. Liu, *Phys. Rev. B* **51**, 11 194 (1995).
- ¹⁹Xiangyang Ma, Lideng Chen, Zhenguo Ji, Hongnian Yao, and Duanlin Que, *J. Phys. Condens. Matter* **7**, 2901 (1993).
- ²⁰Th. Dittrich and V. Yu. Timoshenko, *J. Appl. Phys.* **75**, 5436 (1994).
- ²¹Y. Sakurai, K. Nagasawa, H. Nishikawa, and Y. Ohki, *J. Appl. Phys.* **75**, 1372 (1994).
- ²²J. H. Stathis and M. A. Kastner, *Phys. Rev. B* **35**, 2972 (1987).
- ²³R. Tohmon, H. Mizuno, Y. Ohki, K. Sasagane, K. Nagasawa, and Y. Hama, *Phys. Rev. B* **39**, 1337 (1989).
- ²⁴F. Pio, M. Guzzi, G. Spinolo, and M. Martini, *Phys. Status Solidi B* **159**, 577 (1990).
- ²⁵H. Nishikawa, T. Shiroshima, R. Nakamura, Y. Ohki, K. Nagasawa, and Y. Hama, *Phys. Rev. B* **45**, 586 (1992).
- ²⁶C. C. Koch, *Nanostruct. Mater.* **2**, 109 (1993).
- ²⁷E. Gaffet and M. Harmelin, *J. Less-Common Met.* **157**, 201 (1990).
- ²⁸T. D. Shen, C. C. Koch, T. L. McCormick, R. J. Nemanich, J. Y. Huang, and J. G. Huang, *J. Mater. Res.* **10**, 139 (1995).
- ²⁹E. Gaffet, *Mater. Sci. Eng. A* **136**, 161 (1991).
- ³⁰U. Steinike, B. Müller, I. Ebebt, and H.-P. Hennig, *Krist. Tech.* **14**, 1469 (1979).
- ³¹Shuji Munekuni, Nobuyuki Dohguchi, Hiroyuki Nishikawa, Yoshimichi Ohki, Kaya Nagasawa, and Yoshimasa Hama, *J. Appl. Phys.* **70**, 5054 (1991).
- ³²J. E. Smith, Jr., M. H. Brodsky, B. L. Crowder, M. I. Nathan, and A. Pinczuk, *Phys. Rev. Lett.* **26**, 642 (1971).
- ³³R. Shuker and R. W. Gammon, *Phys. Rev. Lett.* **25**, 222 (1970).
- ³⁴R. J. Nemanich, E. C. Buchler, Y. M. Legrice, R. E. Shroder, G. N. Parsons, C. Wang, G. Lucovsky, and J. B. Boyce, *J. Non-Cryst. Solids* **114**, 813 (1989).
- ³⁵P. M. Fauchet and I. H. Campbell, *CRC Crit. Rev. Solid State Mater. Sci.* **14** (Suppl. 1), S79 (1988).
- ³⁶F. J. Grunthaler, P. J. Grunthaler, R. P. Vasquez, B. F. Lewis, J. Maserjian, and A. Madhukar, *Phys. Rev. Lett.* **43**, 1683 (1979).
- ³⁷P. J. Grunthaler, M. H. Hecht, F. J. Grunthaler, and N. M. Johnson, *J. Appl. Phys.* **61**, 629 (1987).
- ³⁸F. J. Himpsel, F. R. McFeely, A. Taleb-Ibrahimi, J. A. Yarmoff, and G. Hollinger, *Phys. Rev. B* **38**, 6084 (1988).
- ³⁹S. Hasegawa, L. He, T. Inokuma, and Y. Kurata, *Phys. Rev. B* **46**, 12 478 (1992).
- ⁴⁰B. Garrido, J. Samitier, J. R. Morante, J. Montserrat, and C. Dominguez, *Phys. Rev. B* **49**, 14 845 (1994).
- ⁴¹M. Nakamura, Y. Mochizuki, K. Usami, Y. Itoh, and T. Nozaki, *Solid State Commun.* **50**, 1079 (1984).
- ⁴²A. R. H. Cole, *Tables of Wavenumbers for the Calibration of Infrared Spectrometers*, 2nd ed. (Pergamon, New York, 1977), p. 128.
- ⁴³H. A. Szymanski, *Infrared Band Handbook* (Plenum, New York, 1966), Suppl. 3 and 4, p. 67.
- ⁴⁴E. F. Vansant, P. Van Der Voort, and K. C. Vrancken, *Characterization and Chemical Modification of the Silica Surface* (Elsevier, Amsterdam, 1995), p. 59.
- ⁴⁵M. M. Pradhan and M. Arora, *Jpn. J. Appl. Phys.* **31**, 176 (1992).
- ⁴⁶A. Guinier, *X-ray Diffraction* (Freeman, San Francisco, 1963), p. 124.
- ⁴⁷R. Shuker and R. W. Gamon, *Light Scattering in Solids* (Flammarion, Paris, 1971), p. 334.
- ⁴⁸Yoshinori Hibino and Hiroaki Hanafusa, *Appl. Phys. Lett.* **47**, 812 (1985).
- ⁴⁹E. R. Lippincott, A. V. Valkenburg, C. E. Weir, and E. N. Bunting, *J. Res. Natl. Bur. Stand.* **61**, 61 (1958).
- ⁵⁰R. H. Doremus, *Glass Science* (Wiley, New York, 1973).
- ⁵¹J. M. Stevels, *J. Soc. Glass Technol.* **35**, 284 (1991).
- ⁵²D. G. Holloway, *The Physical Properties of Glass* (Wykeham, London, 1973).
- ⁵³T. Takagahara and K. Takeda, *Phys. Rev. B* **46**, 15 578 (1992).
- ⁵⁴L. N. Skuja and A. R. Silin, *Phys. Status Solidi A* **70**, 431 (1982).
- ⁵⁵L. Skuja, *Solid State Commun.* **84**, 613 (1992).
- ⁵⁶S. M. Prokes and O. J. Glembocki, *Phys. Rev. B* **49**, 2238 (1994).
- ⁵⁷S. M. Prokes and W. E. Carlos, *J. Appl. Phys.* **78**, 2671 (1995).
- ⁵⁸L. Z. Zhang, B. Q. Zong, B. R. Zhang, Z. H. Xu, and G. G. Qin, *J. Phys. Condens. Matter* **7**, 697 (1995).
- ⁵⁹P. M. Fauchet, *Phys. Status Solidi B* **190**, 53 (1995).
- ⁶⁰S. Munekuni, N. Dohguchi, H. Nishikawa, Y. Ohki, K. Nagasawa, and Y. Hama, *J. Appl. Phys.* **70**, 5054 (1991).
- ⁶¹A. Shiuger and E. Stefanovich, *Phys. Rev. B* **42**, 9664 (1990).
- ⁶²P. Roura, J. Costa, N. A. Sulimov, J. R. Morante, and E. Bertran, *Appl. Phys. Lett.* **67**, 2830 (1995).